

RESEARCH ARTICLE

Cell Culture and Tissue Engineering

BIOTECHNOLOGY
PROGRESS

Modulation of nutrient precursors for controlling metabolic inhibitors by genome-scale flux balance analysis

Duc Hoang¹  | Bingyu Kuang^{1,2} | George Liang¹ | Zhao Wang¹ |
 Seongkyu Yoon¹ 

¹Department of Chemical Engineering,
 University of Massachusetts Lowell, Lowell,
 Massachusetts, USA

²Bioprocess Development, AbbVie
 Bioresearch Center, Worcester,
 Massachusetts, USA

Correspondence

Seongkyu Yoon, Department of Chemical
 Engineering, University of Massachusetts
 Lowell, Lowell, MA 01854, USA.
 Email: seongkyu_yoon@uml.edu

Funding information

National Science Foundation, Grant/Award
 Number: 1624684; National Institute for
 Innovation in Manufacturing
 Biopharmaceuticals, Grant/Award Number:
 70NANB17H002

Abstract

Therapeutic protein productivity and glycosylation pattern highly rely on cell metabolism. Cell culture medium composition and feeding strategy are critical to regulate cell metabolism. In this study, the relationship between toxic metabolic inhibitors and their nutrient precursors was explored to identify the critical medium components toward cell growth and generation of metabolic by-products. Generic CHO metabolic model was tailored and integrated with CHO fed-batch metabolomic data to obtain a cell line- and process-specific model. Flux balance analysis study was conducted on toxic metabolites cytidine monophosphate, guanosine monophosphate and n-acetyl-putrescine—all of which were previously reported to generate from endogenous cell metabolism—by mapping them to a compartmentalized carbon utilization network. Using this approach, the study projected high level of inhibitory metabolites accumulation when comparing three industrially relevant fed-batch feeding conditions one against another, from which the results were validated via a dose-dependent amino acids spiking study. In the end, a medium optimization design was employed to lower the amount of supplemented nutrients, of which improvements in critical process performance were realized at 40% increase in peak viable cell density (VCD), 15% increase in integral VCD, and 37% increase in growth rate. Tight control of toxic by-products was also achieved, as the study measured decreased inhibitory metabolites accumulation across all conditions. Overall, the study successfully presented a digital twin approach to investigate the intertwined relationship between supplemented medium constituents and downstream toxic metabolites generated through host cell metabolism, further elucidating different control strategies capable of improving cellular phenotypes and regulating toxic inhibitors.

KEY WORDS

culture medium development, fed-batch bioprocess, flux modeling simulation, metabolic inhibitors, metabolic shift, therapeutic protein production

1 | INTRODUCTION

Duc Hoang and Bingyu Kuang contributed equally to this work.

Biotherapeutics are of key importance for treatment of many diseases including cancers and autoimmune disorders. Chinese hamster ovary

(CHO) cells represent the most widely used host cell for therapeutic recombinant protein production.¹ CHO expression hosts are characterized by their high nutrients uptake rate during cellular expansion and production phase. However, inefficient intracellular metabolism often prevents cells to fully utilize nutrients to support growth and protein production. Instead, a significant fraction of fed glucose and amino acids are diverted into generation of toxic metabolites.^{2,3} Owing to this, tandem liquid chromatography-mass spectroscopy (LC-MS/MS) has emerged as one of the most powerful set of tools for various metabolomic studies due to its capability of analyzing countless of metabolites and medium additives from a single sample.^{4,5} These advances in metabolomics have enabled identification of additional cell generated inhibitory metabolites, other than lactate and ammonia.⁶ In our most recent work, it has been shown that untargeted global metabolomics coupled LC-MS/MS can be applied to batch and fed-batch CHO bioprocess to identify six growth and titer production metabolic inhibitors generated from CHO metabolism.⁷

Constraint-based flux balance analysis (FBA) is a computational approach to study metabolic networks.^{8,9} Coupled with a metabolic model network comprising of biochemical reactions capable of composing cell metabolism, FBA can be employed to examine metabolic systems of various organisms. As such, a recent study showed the capability of tailoring the generic CHO GEM into host and recombinant cell-specific model to understand the genotypic and phenotypic traits differences between wild type and recombinant cells.¹⁰ Others successfully combined *in silico* modeling and metabolomic analysis to characterize fed-batch of CHO cultures.¹¹

Despite contributing to the overall fundamental understanding of CHO cell metabolism, these studies often remain singular, and the mechanisms underlying cellular metabolic shift under different process conditions, as well as the metabolic relationships between toxic by-products and feeding nutrients in CHO intracellular network are not yet fully understood. In this study, a digital twin approach was presented to optimize CHO bioprocess by integrating *in silico* flux balance analysis with process optimization. Generic CHO-K1 metabolic model was tailored and further integrated with CHO fed-batch metabolomic data to obtain a cell line- and process-specific model. Metabolic by-product cytidine monophosphate (CMP), guanosine monophosphate (GMP) and *n*-acetylputrescine (NAP), all of which previously reported to generate from endogenous cell metabolism and verified to be toxic to cells,^{7,12} were further mapped to a compartmentalized carbon utilization network. Flux balance analysis was conducted at both the genome-scale level and simplified carbon utilization network level to gain a deeper mechanistic understanding in generation of toxic metabolites and to identify the critical medium components toward cell growth and generation of metabolic by-products. The study established an *in silico* metabolomic platform relating metabolic inhibitors with their nutrient precursors, which were further experimentally validated based on an amino acid dose-dependent spiking study. The data obtained from the study altogether enabled visualization of the intertwined relationship

between supplemented medium constituents and downstream toxic metabolites generating through host cell metabolism, providing a deeper mechanistic understanding into different CHO physiologies in response to process input parameters, with applications spanning from cell line evaluation, metabolic engineering to media optimization and biomanufacturing control.

2 | MATERIALS AND METHODS

2.1 | Cell line, media, and supplements

A CHO-K1 cell line expressing IgG (VRC01) antibody from NIH (National Institute of Health) was used for this study with two proprietary media. For inoculation, basal medium (medium A) from MilliporeSigma (Burlington, MA, USA) and glutamine at 6 mM (unless otherwise stated) from Corning (Corning, NY, US) were supplemented to cell culture on Day 0. For fed-batch process, enriched nutrient feed medium (medium B) from Lonza (Portsmouth, NH, USA) was used as feed medium and fed to cells after Day 0 until cell viability dropped below 80%. The initial feeding day was dependent on the development of feeding strategy and was addressed where appropriate throughout the discussion. Cells were cultivated in sterile 125 ml shake flask from Fisher Scientific (Waltham, MA, USA) with a working volume of 30 ml in a humidified, shaking incubator (Model AJ125) from ATR Biotech (Laurel, MD, USA) operated at 125 RPM, 36.5°C, and 5.2% carbon dioxide. For the fed-batch feeding study, a bolus of either 5%, 10% or 15% of the initial feeding volume was administered daily to cells. Cells were inoculated at low viable cell density (VCD) (approximately 0.5×10^6 cells/ml) in basal medium and harvested when cell viability dropped below 80%. Sub-culturing was done every 2 to 3 days when the cells reached VCD greater than 3×10^6 cells/ml. Cell viability was maintained above 90% throughout the inoculation phase.

2.2 | Assessment of growth and productivity

VCD and viability were measured daily with a cell counter device (CeDex HiRes) from Roche (Branchburg, NJ, USA). Glucose, lactate, and ammonia concentration data from each culture condition were measured using a benchtop analyzer (Bioprofile FLEX) from Nova Biomedical (Waltham, MA, USA). Titer analysis was performed using a high-pressure liquid chromatography (HPLC) system (Agilent 1100 series) obtained from Agilent Technologies (Santa Clara, CA, USA) with a protein A column (Poros A, 2 μ m, 2.1 \times 30 mm) obtained from Thermo Scientific (Waltham, MA, USA). Cell culture supernatant samples were collected daily for metabolomic analysis. The integral viable cell density (IVCD) at day n was defined as the summation of VCD for each day during CHO cell culture up until day n . To compare and evaluate the performance of each culture condition, the productivity at day n was calculated—defined as the overall measured titer (g/L) obtained at day n .

2.3 | LC-MS samples preparation

LC-MS grade chemical solvents and reagents from MilliporeSigma were used as buffers for all LC-MS analysis. Amino acid standards also from MilliporeSigma were used for quantification of residual amino acid measurements in the spent medium. For internal standard solution preparation, isotopic labeled amino acid standards set A (NSK-A) from Cambridge Isotope Laboratories (Andover, MA, USA) was dissolved in water to the appropriate concentration. Each sample was prepared by mixing 10 μ l of sample with a matrix containing 10 μ l culture medium, 10 μ l IS and 30 μ l acetonitrile. Samples were vortexed for 30 s and centrifuged for 20 min at 16,000 g. The supernatant was then extracted for LC-MS analysis. For inhibitory metabolites analysis, inhibitory metabolite standards were purchased from MilliporeSigma. Isotopic labeled internal metabolite standards were purchased from Toronto Research Chemicals.

2.4 | LC-MS samples analysis

Analysis of cell culture sample was performed using 2 μ l sample injecting to an ACQUITY UPLC instrument from Waters (Milford, MA, USA) coupled with a quadrupole time-of-flight Xevo G2-XS mass spectrometer also from Waters. For amino acid analysis, LC separation was performed on a normal phase column (Intrada, 3 μ m, 100 \times 3 mm) manufactured by IMTAKT (Portland, OR, USA). For LC condition, the gradient program was set at 20% A (0–4 min), 100% A (4–14 min), 100% A (14–17 min), 20% A (17–20 min) at 0.4 ml/min. For inhibitory metabolites analysis, LC separation was performed on a PEEK coated column (SeQuant ZIC-cHILIC, 3 μ m, 100 \times 2.1 mm) with a guard kit (SeQuant ZIC-cHILIC, 5 μ m, 20 \times 2.1 mm), both obtained from Millipore Sigma. The elution program was set at: 10% A (0–0.5 min), 30% A (2.5–5.5 min), 45% A (5.5–7.0 min), 65% A (7.0–10.0 min), 10% A (10.1–14.0 min). For MS analysis, mass range was set to 50–1200 Da with scan time of 0.5 s in centroid mode. Mass detection was performed in both positive and negative polarity under sensitivity mode. Leucine-enkephalin (leu-enk) was applied as lock mass reference for accurate mass calibration to counteract the potential effect of calibration drift during the long analytical sequences run time. For leu-enk lockspray setup, the following parameters were applied: positive mass 556.2771 Da; negative mass 554.2615 Da; scan time 0.5 s; scan interval 30 s; mass window \pm 0.5 Da. For MS settings, the following parameters were used for electrospray ionization (ESI): capillary voltage 3.0 kV; sampling cone 40 V; source offset 80 V; source temperature 100°C; desolvation temperature 20°C; cone gas 40 L/h; desolvation gas 600 L/h.

2.5 | Gene expression analysis through real-time polymerase chain reaction

Gene expression analysis was conducted through quantitative real-time polymerase chain reaction (qPCR) using SYBR Green-based

detection on a 7500 real-time PCR system by Applied Biosystems (Waltham, MA, USA). For qPCR, cocktail composition for one reaction was as follows: 2 \times SYBR Green master mix (10 μ l), 10 \times forward/reverse primers (2 μ l), RNase-free water (4 μ l), and diluted sample (4 μ l). Final volume for each cocktail was 20 μ l. Detail cycling parameters were set as follows: one cycle of initial denaturation (per cycle: 94°C-2 min); 45 cycles of polymerization (per cycle: 94°C-15 s, 56°C-1 min, 72°C-1.5 min); 1 cycle of final extension (per cycle: 72°C-5 min); 1 cycle of hold (per cycle: 4°C-20 s).

2.6 | Flux modeling and flux balance analysis

During cell expansion phase, it can be expected that cells follow closely to a linear growth model. Assuming CHO cells growing exponentially, the metabolite exchange rates r (mmol/h) can be estimated by evaluating the change in measured concentration of metabolite i [C_i] (mmol) over time:

$$r = \frac{d[C_i]}{dt} \quad (1)$$

Assuming CHO cells growing exponentially, r can be estimated by evaluating the change in C_i over time:

$$r = \frac{d[C_i]}{dt} \approx \frac{\Delta C_i}{\Delta t} \quad (2)$$

The foundation of FBA assumes the metabolism of a single cell is defined by a system of n reactions.¹³ The limiting steady state assumption of FBA at equilibrium condition ($t \rightarrow \infty$) constrains the fluxes within an average, single cell \hat{c} consumed by FBA so that:

$$\frac{d[\hat{C}_i]}{dt} = \sum_{j=1}^n S_{ij}^c \hat{\nu}_j^c = 0, \forall i. \quad (3)$$

Here, S_{ij} is the stoichiometric coefficient for metabolite i in reaction j and the flux of reaction j is ν_j . FBA is predicated on the assumption that cells have been tuned through a biochemical exchanging process to a stage where they “optimally” utilize their resources, where “optimal” is measured by a function of the fluxes, $g(\nu)$. Hence, FBA studies metabolic processes through optimization problem of the form:

$$\max \{g(\hat{\nu}): \hat{S}^c \hat{\nu}^c = 0, \hat{L}^c \leq \hat{\nu}^c \leq \hat{U}^c\}, \quad (4)$$

where \hat{S}^c is the stoichiometric matrix of components S_{ij} . The objective function $g(\nu)$ is defined to be the rate at which biomass is created. For convenience, $g(\nu)$ is assumed to only contain the sole flux of the growth reaction (i.e., $g(\hat{\nu}^c) = \nu_{\text{growth}}$). The vectors of lower bounds (\hat{L}^c) and upper bounds (\hat{U}^c) may contain fluxes of value approaching infinity, or some suitably large value, indicating that at a flux is

unbounded. If both $\hat{L^c} < 0$ and $\hat{U^c} > 0$, then the biochemical reaction is said to be reversible. In this study, where appropriate, FBA was conducted based on a CHO-K1 specific genome scale model previously published.¹⁴

2.7 | Growth and exchange rate calculation

In this study, a compartmentalized carbon metabolic model of CHO cells was adapted from a previous publication.¹⁵ To describe biomass, a lumped equation which comprised of different anabolic requirements for cells was used.¹⁵ The dry weight mass of cells was assumed to be 0.315 mg/cells, as previously described.¹⁶ In this study, additional metabolic equations describing generation of metabolic inhibitor CMP, GMP and NAP were also amended to the model, of which FBA data fitting was conducted to describe fluxes diverting into inhibitory metabolite pathways.

2.8 | Growth and exchange rate calculation

Growth rates of CHO cells were assumed to follow exponential growth behavior:

$$N_x = N_{x,0} \times e^{\mu t}. \quad (5)$$

Here $N_{x,0}$ ($\times 10^6$ cells/ml) is the number of cells at time 0 (h), N_x ($\times 10^6$ cells/ml) is the number of cells after culture time t (h). The IVCD profile of cell at time t_n can be calculated as followed:

$$\text{IVCD}_{t_n} = \text{IVCD}_{t_{n-1}} + \frac{(\text{VCD}_{t_n} + \text{VCD}_{t_{n-1}})}{2} \Delta t. \quad (6)$$

Rearranging (5), cell growth rate μ (h^{-1}) therefore can be expressed as a log-based growth model:

$$\mu = \frac{\ln(N_x/N_{x,0})}{t}. \quad (7)$$

3 | RESULTS AND DISCUSSION

3.1 | Design of fed-batch feeding process on CHO-K1 cell line

CHO cells are known to consume large amount of substrates during growth and production, inefficient endogenous metabolism prevents cells to fully utilize fed nutrients. As an effort to understand and investigate into cellular metabolic shift, a high-cell-density (HCD) fed-batch feeding study with three different feeding conditions on a CHO-K1 cell line using medium A were conducted, as illustrated in Table 1.

TABLE 1 Culture feeding strategy for high cell density process development

Condition	Feeding volume (% seed volume)
Low feed	Low–5% (1.5 ml feeding)
Medium feed	Medium–10% (3 ml feeding)
High feed	High–15% (4.5 ml feeding)

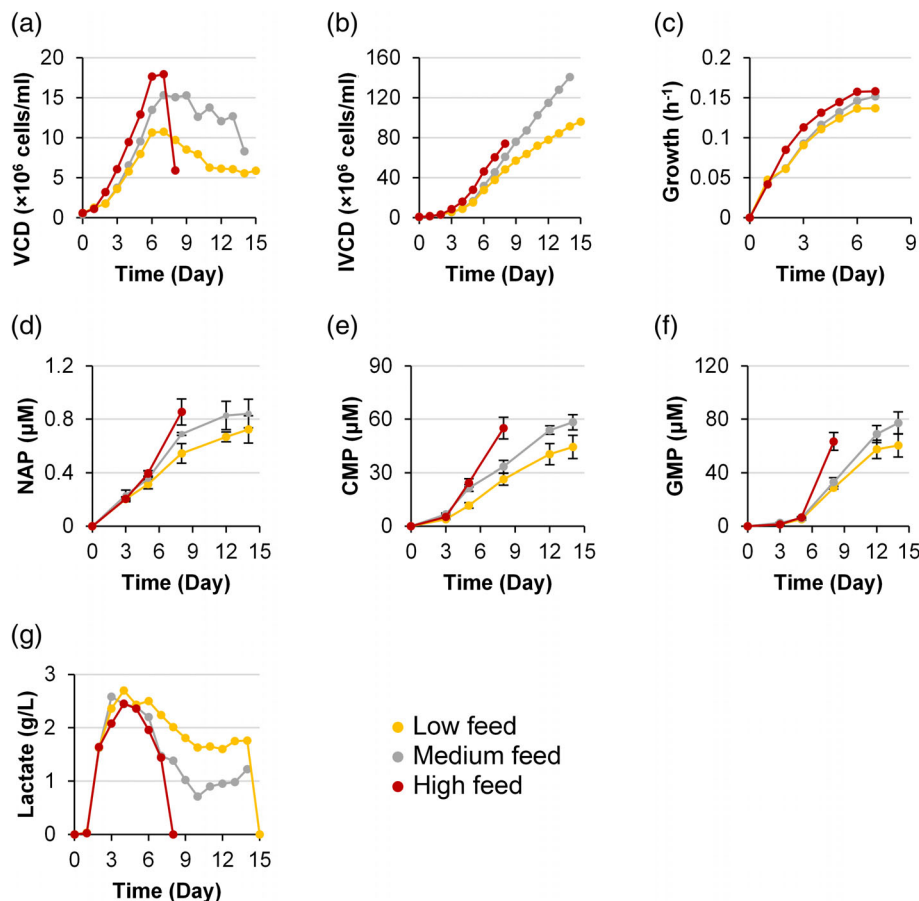
Note: Feeding strategy was designed and referenced to the inoculation seeding volume (30 ml).

In summary, when studied the effect of different feeding volumes on cell culture performance, the results from the study showed that high feed (4.5 ml feeding, starting on Day 2) resulted in the highest peak VCD on Day 7. Interestingly, peak VCD also directly correlated to shortest culture duration, as cell viability the high feed condition crashed rapidly the following days (starting on Day 8) when compared against the other conditions. On the other hand, low feed volume, despite showing the longest culture duration, generally suffered from relatively low peak VCD (see Figure 1a). A similar trend was also observed from the IVCD and growth rate profile of cells, as both low and high feeding volumes similarly resulted in worse cellular performance (Figure 1b,c). Accumulation profile of process inhibitors including lactate and other amino acids and sugar derived metabolites were also shown (Figure 1d–g). Interestingly, despite stark differences when comparing their phenotypes, peak lactate accumulation due to different feeding strategies did not show significant differences. However, accumulation patterns of toxic metabolites CMP, GMP and NAP were all found to be increased with respect to the volume of daily feed administered. It could be speculated that up-regulated metabolic activities due to excess supplemented nutrients can negatively impact culture performance, suggesting that a deeper investigation into cell metabolism is needed to understand cellular allocation of fed resources to support growth or diverting into non-optimal pathways. Overall, the study showed that nutrients-rich feeding in fed-batch process, although classically aiming to maximize resource use and keeping cells from depriving of nutrients in high-cell-density culture, in this case allowing cells to over-consume than the required amount necessary for growth and divert most of them toward generation of metabolic byproducts, some of which are cytotoxic.

3.2 | Development of inhibitory metabolites control strategy via simplified central carbon utilization network

CHO cell metabolism can be described by a network consisting of hundreds of enzymes catalyzed biochemical reactions.¹⁴ In this approach, a simplified carbon utilization network was employed to systematically assess the relationships between host cell metabolism and generation of metabolic process inhibitors. To achieve this, different putative metabolic pathways generating inhibitory metabolites

FIGURE 1 Cellular phenotype characteristic and inhibitory metabolite time-course profiles of fed-batch CHO-K1 cells. Time-course phenotype characteristic profiles: (a) viable cell density (VCD), (b) cumulative increase in integral VCD (IVCD), and (c) growth rate. Time-course inhibitory metabolite profiles: (d) n-acetylputrescine (NAP), (e) cytidine monophosphate (CMP), (f) guanosine monophosphate (GMP), and (g) lactate. Fed-batch study of CHO-K1 cells were conducted at 0.5×10^6 cells/ml seeding density in 30 ml culture volume. For all conditions, the initial seeding day was assigned to be Day 0. Three different feeding volume strategies were employed: low feed (5% seed volume feeding), medium feed (10% seed volume feeding), and high feed (15% seed volume feeding). Cells from all conditions were derived from the same culture to eliminate variation in growth cycle and other culture conditions due to batch-to-batch variation



were mapped to a simplified carbon utilization network of cells (Figure 2a). Specifically, metabolite CMP can be generated as the downstream product through the condensation reaction between 5-phosphoribosyl diphosphate (PRPP, intermediate of glycolysis pathway) and orotic acid (ORA, intermediate of glutamine metabolism). Neighboring to CMP, metabolite GMP can also be directly synthesized from PRPP. On the other hand, metabolite NAP was identified as downstream product from the metabolism of glutamine, arginine, and proline, respectively. Metabolomic data together with the measured growth rate data obtained from the previously conducted fed-batch study were used to fit intracellular fluxes during cell expansion phase. Comparison of flux distribution between low feed, medium feed and high feed conditions was conducted through a simplified compartmentalized carbon utilization network. Metabolic fluxes were then assessed by conducting flux balancing analysis using the measured uptake rates as constraints. Representation of cellular fluxes diverting into forming toxic metabolites using flux balancing analysis framework was shown in Figure 2b-g. Metabolic fluxes diverted toward generating inhibitory by-products were all found to be highest in the case of high feed condition, followed by medium and low feed. The study suggested that higher consumption rate of substrates, such as amino acids and glucose, although were experimentally measured to be higher, did not translate to better culture performance, but instead gravitating toward generation of previously identified toxic by-products into the cytoplasm compartment of cells.

3.3 | Design of dose-dependent nutrients spiking study

As an effort to control and optimize the cellular phenotype in a standard CHO bioprocess, a dose-dependent nutrients spiking study was designed to identify and validate key medium constituent precursors upstream to the formation of metabolites. In this study, glutamine, proline, and glucose which were previously explored in the *in silico* flux simulation study at the simplified carbon compartmentalized network level (see Figure 2) were evaluated for their impact on downstream inhibitor generation. Other amino acids potentially involve in the generation of inhibitors via distant or indirect pathways (such as arginine and aspartate regarding generation of CMP and GMP, or aspartate regarding the generation of NAP) were also investigated in this study. Schematic diagram mapping downstream toxic metabolites to upstream nutrients was also shown (see Figure 3a). In this study, targeted amino acids were divided into two groups. For group 1 (G1) targeting metabolite CMP and GMP, a bolus consisted of arginine, aspartate, glucose and glutamine were supplemented to cells on Day 0 in addition to the inoculated basal medium. For group 2 (G2) targeting metabolite NAP, only proline was added to cells along with the basal medium. For each group, two different factors were tested. The concentration of each added substrate was spiked at either two-factor (2 \times) or three-factor (3 \times) higher than the concentration of the control (no spiking, same as basal medium). For both spiking conditions, pure

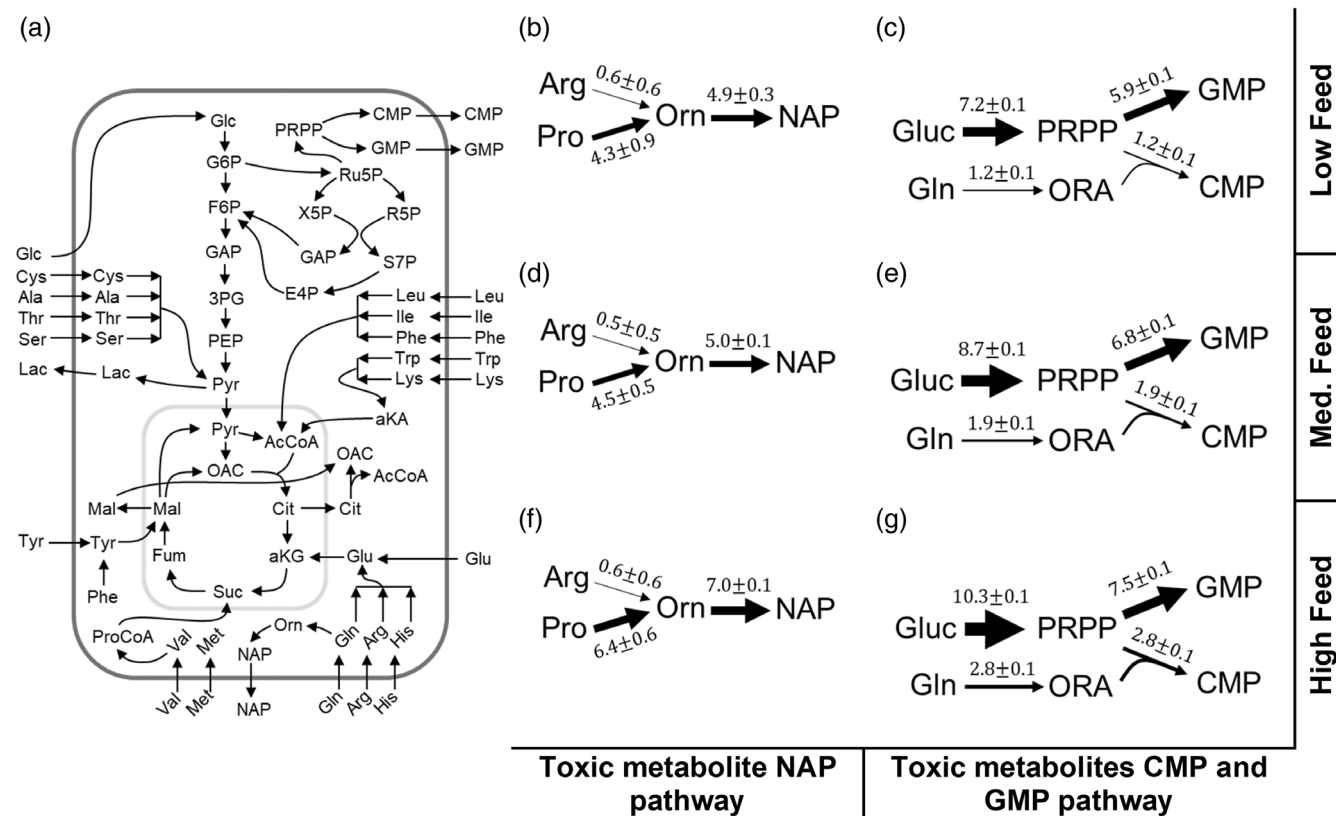


FIGURE 2 Analysis of flux diverting into toxic metabolites pathway via metabolomics data fitting framework. (a) Compartmentalized carbon network utilized for flux analysis study. (b,d,f) Simulation of fluxes diverting to generate toxic metabolite n-acetylputrescine (NAP) through glutamine, arginine, and proline metabolism under different feeding conditions. (c,e,g) Simulation of fluxes diverting to generate toxic metabolites cytidine monophosphate (CMP) and guanosine monophosphate (GMP) through glucose and glutamine metabolism under different feeding conditions. In this study, metabolic pathways generating process inhibitors were mapped to CHO central carbon utilization network. Metabolic fluxes and flux variability analysis were assessed by fitting metabolomics uptake rates and growth rate data to the core model of cells. Flux, $\mu\text{mol}/10^6 \text{ cells}/\text{h}$; Arg, arginine; CMP, cytidine monophosphate; Gln, glutamine; Gluc, glucose; GMP, guanosine monophosphate; NAP, n-acetyl putrescine; ORA, orotic acid; Pro, proline; Orn, ornithine; PRPP, 5-phosphoribosyl diphosphate

substrates were dissolved in minimum level of water to prepare concentrated stock spiking solution and administered to cells. Dissolving substrates in pure water (and not medium solution) prevents introduction of other nutrients typically found in enriched medium which introduces additional factors that cannot be controlled. The exact dose amount of each substrate from each condition as spiked into CHO-K1 fed-batch cultures can be found in Figure 3.

3.4 | Phenotype results of dose-dependent nutrients spiking study

In this dose-dependent nutrients spiking study, cells were grown over the course of 14 days, of which cellular phenotypes and various performance characteristics were measured and evaluated (see Figures 4 and 5). Critical process performance (CPP) attributes of the conditions with excess nutrients spiked in on Day 0 were compared against the control group. Unsurprisingly, intensified nutrients spiking at both 2 \times and 3 \times concentration over the control (G1-2 \times , G1-3 \times , G2-2 \times , and G2-3 \times) all resulted in decreased performance of cells. In general, it

was observed that all experimental conditions spiked excess substrates showed inhibition on cell growth during both exponential and stationary phase of the culture process. Specifically, peak VCD of cells realized a 4.1% decrease and 18.7% decrease when spiked at two times (G1-2 \times) and three times (G1-3 \times), respectively, when compared against the control (see Figure 4a). Other culture characteristics, such as IVCD and growth rate, were also observed to be consistently lower throughout the entire culture duration at 11.5% IVCD and 11.8% growth rate decrease for G1-2 \times , and further exacerbated at 21.8% IVCD and 17.6% peak growth rate decrease for G1-3 \times (see Figure 4b,c). Interestingly, negative impact on cell culture performance at two times spiking for group 2 (G2-2 \times) was not as significant as three times spiking (G2-3 \times , see Figure 5a-c). These findings were consistent with the results from another study which reported that spiking of NAP back into cell culture at millimolar level did not seem to show toxic effect on the growth of cells.⁷ It was speculated that the observation as shown here, along with the data previously reported in other studies, suggested that NAP was re-directed into the arginine metabolism pathway. Specifically, NAP potentially can be converted back to putrescine which is a substrate from the polyamine

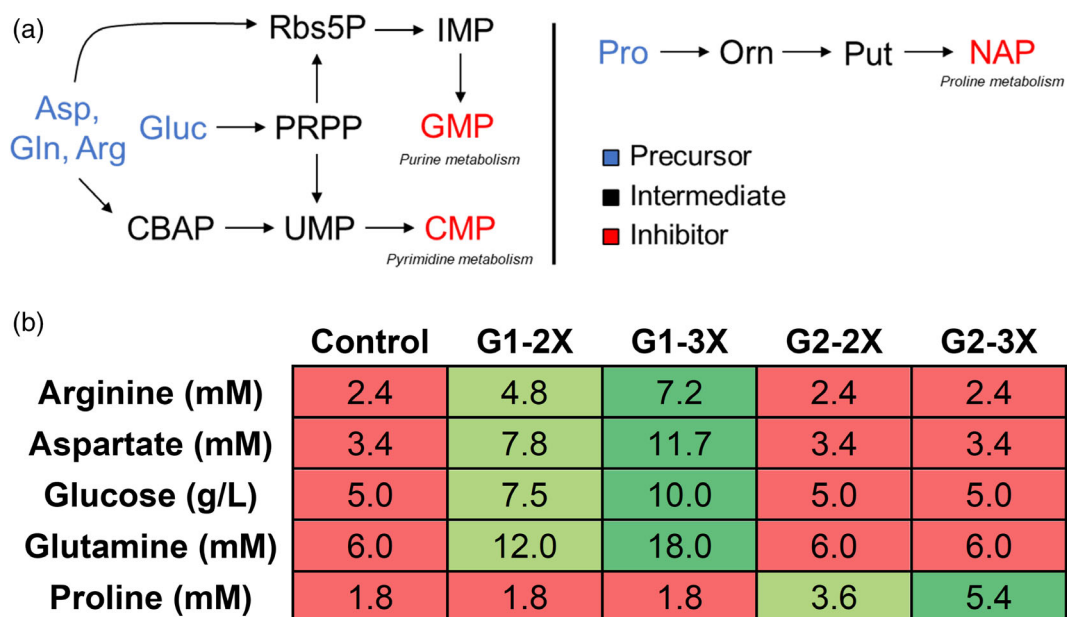


FIGURE 3 Schematic diagram of inhibitory metabolites-related metabolic pathways and design of dose-dependent nutrients spiking study conducted on CHO-K1 cells. (a) Schematic diagram of cellular metabolic network correlating downstream toxic metabolites to upstream nutrient precursors. (b) Design of amino acids dose-dependent nutrients spiking study. The study was divided into two groups. For group 1 (G1), arginine, aspartate, glucose, and glutamine were supplemented to cells on Day 0 in addition to the inoculated basal medium. For group 2 (G2), only proline was tested. In this analysis, each condition was spiked with two different levels of substrates, either at two-factor (2×) or three-factor (3×) higher than the concentration as found in the control. For both spiking conditions, pure substrates were dissolved in minimum level of water to prepare stock spiking solution and administered to cells. Arg, arginine; Asp, aspartate; CBAP, carbamoyl phosphate; CMP, cytidine monophosphate; Gln, glutamine; Gluc, glucose; GMP, guanosine monophosphate; IMP, inosine monophosphate; NAP, *n*-acetyl putrescine; Orn, ornithine; Pro, proline; PRPP, 5-phosphoribosyl diphosphate; Put, putrescine; Rbs5P, 5-phosphoribosylamine; UMP, uridine monophosphate

pathway which generates growth factors to promote cell proliferation in mammalian systems¹⁷ and therefore neutralizing the inhibitory effect of NAP on cell growth. Alternatively, excess NAP could also drive the metabolic flux in the forward direction downstream of its formation and can be further utilized by cells to support proliferation. At 3× spiking level, however, the inhibitory effect of NAP on cellular performance was apparent, at cells realized a 16.2% decrease in VCD, 8.7% decrease in total IVCD and 17.6% decrease in peak growth rate (see Figure 5a–c). Due to the apparent reduction in various CPP observed across all tested conditions as shown here, the study next sought to evaluate the accumulation of process inhibitors at different substrate spiking conditions as well as the titer production profile to better understand the correlation between excess nutrients and their impact on various important process parameters.

A major challenge of mammalian bioprocess is the generation of unwanted toxic by-products during growth and protein production phase of cell culture. This is mostly due to the prolonged nature of a standard industrial culture bioprocess; cells are often exposed to toxic metabolites for an extended period under bench-scale fed-batch study or pilot-scale bioreactor process with long culture duration. The accumulation profile of process inhibitors was therefore profiled throughout the culture to establish a linkage between metabolites generated during metabolism of cells and other important CPP attributes (see Figures 4d–g and 5d–f). When investigating into the

accumulation profile of various process inhibitors, it was found that the accumulation profile of lactate and ammonia only from G1 cells increased as the spiking concentration of nutrients increased. Historically, lactate is known as by-product when glucose is metabolized into pyruvate, and hence higher input glucose concentration can explain for the observed higher measured lactate concentration (see Figure 4f). Higher accumulated concentration of ammonia was also expected, as ammonia is typically produced through the metabolism of nitrogen-contained amino acid (in this case, glutamine). Unsurprisingly, this behavior was not found in G2 spiking where no significant differences were found in both lactate and ammonia profiles across all G2 cells (see Figure 5e), mostly due to both glucose and glutamine of all experimental conditions were kept at the same level as the control (see Figure 3). Unsurprisingly, conditions spiked with excess substrates (2× and 3× spiking) all showed higher accumulation of process inhibitors in the extracellular environment across the entire culture duration when compared against the control. Regarding 2× versus 3× spiking conditions, the data obtained from the study revealed that high level spiking (3×) consistently generated higher concentration of inhibitors. Interestingly, when comparing the 2× and 3× spiking conditions one against the other, the concentration of CMP and GMP from was shown to be distinctively different during the early days of the culture but appeared to be equal at the harvest day (Day 14, Figure 4d,e). Historically, and unlike some other end-product

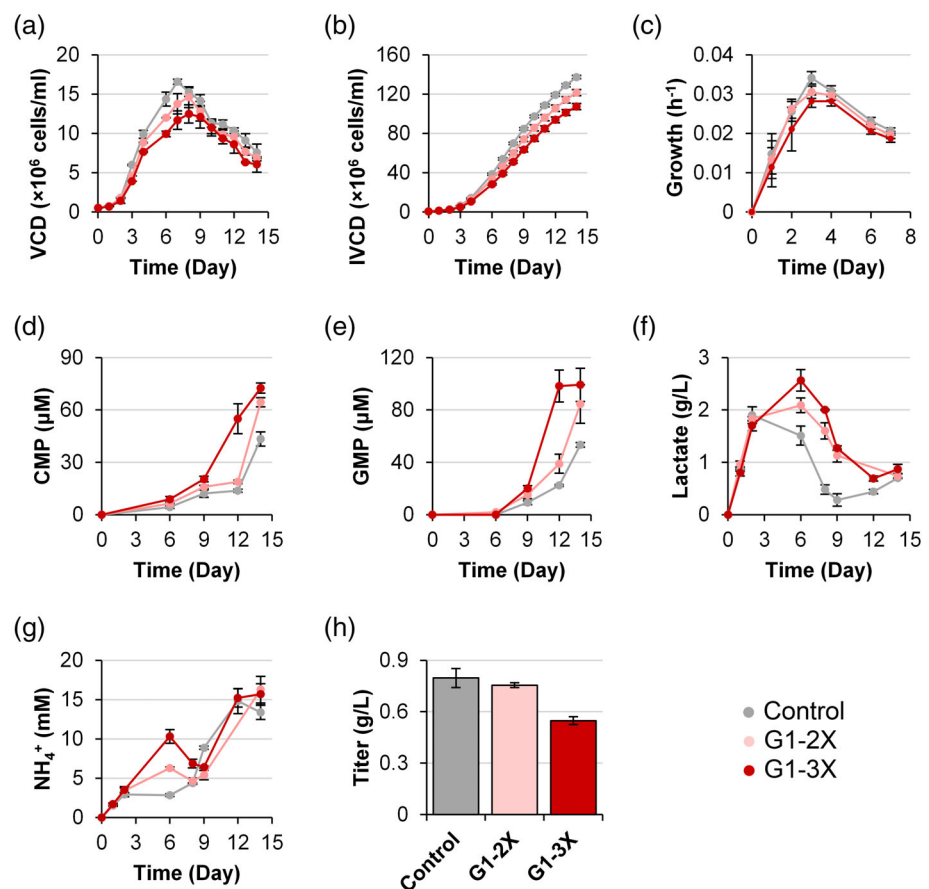


FIGURE 4 Cellular phenotype characteristic and inhibitory metabolite time-course profiles of group 1 (G1) fed-batch CHO-K1 cells obtained from dose-dependent nutrients spiking study. Time-course phenotype characteristic profiles: (a) viable cell density (VCD), (b) cumulative increase in integral viable cell density (IVCD), and (c) growth rate. Time-course inhibitory metabolite profiles: (d) cytidine monophosphate (CMP), (e) guanosine monophosphate (GMP), (f) lactate, and (g) ammonia. Also shown: (h) titer profile obtained at the harvest day of the cultures. Fed-batch study of CHO-K1 cells were conducted at 0.5×10^6 cells/ml seeding density in 30 ml culture volume. For all conditions, the initial seeding day was assigned to be Day 0. For G1 cells, excess doses of arginine, aspartate, glucose, and glutamine (2 \times and 3 \times) were spiked into the cultures on Day 0. Cells from all conditions were derived from the same culture to eliminate variation in growth cycle and other culture conditions due to batch-to-batch variation. Cellular phenotype characteristics and toxic metabolites accumulation profile were evaluated to assess the impact of excess nutrients spiking dosage on overall performance of cells. 2 \times , two-factor spiking of substrates; 3 \times , three-factor spiking of substrates

metabolites which cannot be efficiently utilized by cells (such as ammonia), CMP and GMP can both be metabolized by cells as monomers toward RNA production. In this case, it could be hypothesized that cells have internally allocated metabolic resources toward adapting a higher metabolism of CMP and GMP as a response to mediate the effect of excess CMP and GMP generation, which consequentially came at a cost of lower overall process performance.

Monoclonal antibody production of cells obtained at harvest day from the dose-dependent nutrients spiking study was also evaluated. Overall, cultures spiked with 2 \times and 3 \times substrate concentration all showed decrease in titer production when compared against the control. Specifically, for group 1 targeting metabolite CMP and GMP, 2 \times feeding condition realized a 5.2% decrease in titer production when compared against the control. This was further exacerbated at 3 \times feeding level where cells showed up to 31.2% decrease in titer profile. A similar trend was also observed for group 2 of the study targeting metabolite NAP where 2 \times spiking condition realized a 12.8% and 17% decrease in total

titer production at 2 \times and 3 \times level, respectively. This observation as shown here, coupled with the remarks as shown previously with inferior cellular phenotypic profile in conditions with high level of process inhibitors accumulated, altogether further confirming the strong correlation between the supplemented pool of nutrients to the downstream formation of metabolites as previously explored in the *in silico* flux modeling study, while also suggesting that optimizing medium constituents, specifically to lower the supplemented concentration of certain key substrates, may improve overall cell growth profile.

3.5 | Gene expression results of dose-dependent nutrients spiking study

Downstream metabolic genes involved in CMP-related metabolic pathway nested in the pyrimidine metabolism and their respective

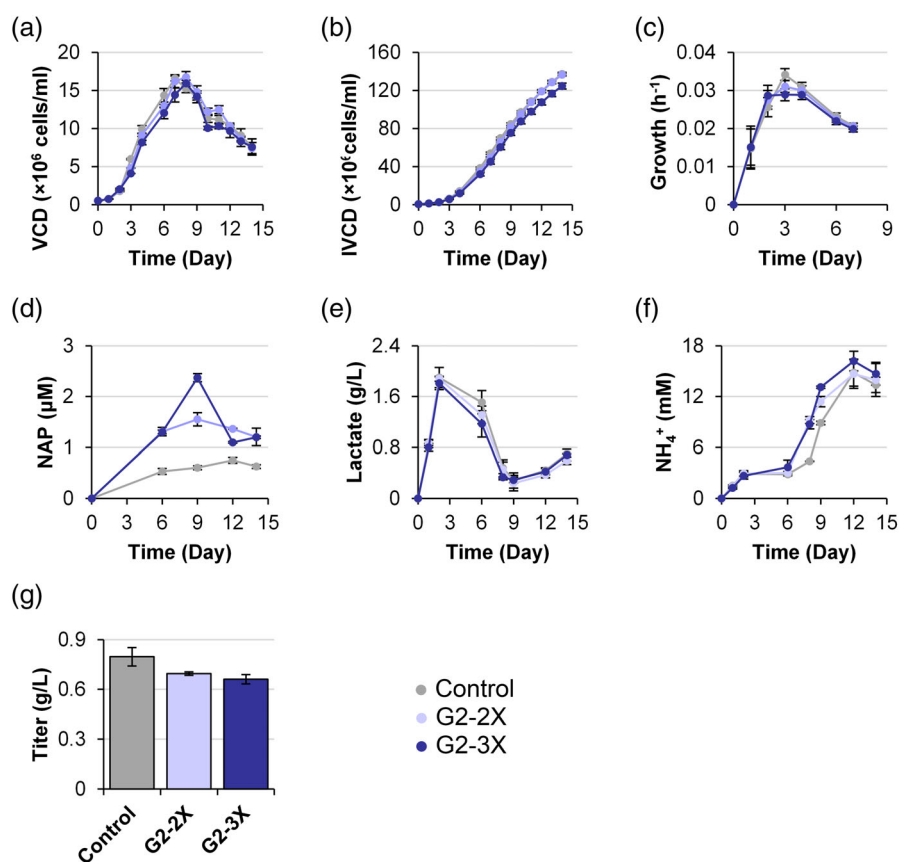


FIGURE 5 Cellular phenotype characteristic and inhibitory metabolite time-course profiles of group 2 (G2) fed-batch CHO-K1 cells obtained from dose-dependent nutrients spiking study. Time-course phenotype characteristic profiles: (a) viable cell density (VCD), (b) cumulative increase in integral viable cell density (IVCD), and (c) growth rate. Time-course inhibitory metabolite profiles: (d) n-acetylputrescine (NAP), (e) lactate, and (f) ammonia. Also shown: (g) titer profile obtained at the harvest day of the cultures. Fed-batch study of CHO-K1 cells were conducted at 0.5×10^6 cells/ml seeding density in 30 ml culture volume. For all conditions, the initial seeding day was assigned to be Day 0. For G2 cells, excess doses of proline (2 \times and 3 \times) were spiked into the cultures on Day 0. Cells from all conditions were derived from the same culture to eliminate variation in growth cycle and other culture conditions due to batch-to-batch variation. Cellular phenotype characteristics and toxic metabolites accumulation profile were evaluated to assess the impact of excess nutrients spiking dosage on overall performance of cells. 2 \times , two-factor spiking of substrates; 3 \times , three-factor spiking of substrates

enzyme expression level evaluated via qPCR were also studied (see Figure 6a). Fed nutrients including glutamine generated from alanine and aspartate metabolism act as substrate to generate n-carbamoyl-l-aspartate (CBAP), which is further metabolized into CMP. Uridine-cytidine kinase 2 (*Uck2*) facilitates the conversion of CMP to cytidine which is further metabolized into β -alanine (β -Ala). Ultimately, β -Ala is converted to acetyl coenzyme A (AcCoA) toward energy production in the citric acid cycle via 4-aminobutyrate aminotransferase (*Abat*). Downstream metabolite cytidine can also be reversely synthesized to CMP through 5'-nucleotidase (*Nt5*). Thus, elevated enzymatic expression level of *Uck2*, *Nt5*, and *Abat* can serve as strong indication of excess CMP accumulated as response to mediate cytotoxic stress imposed by the dose-dependent nutrients spiking study due to excess accumulation waste metabolites.

The gene expression levels of *Uck2*, *Nt5*, and *Abat* as expressed on Day 3, Day 12, and Day 14 along with the corresponding pair of forward and reverse primers as quantified via qPCR are shown in Figure 6b–e. In general, the results showed a higher expression level of

Uck2, *Nt5*, and *Abat* from the substrates spiking conditions across all days when compared against the control, suggesting an increasing accumulation pattern of CMP as cells continuously metabolizing fed substrates. Interestingly, the expression level of *Uck2*, and especially *Nt5*, gradually increased toward the end of the culture (see Figure 6c,e). Tracing back to the schematic pathway diagram (see Figure 6a), *Uck2* and *Nt5* were found to be the direct downstream genes in relative to CMP. Increasing level of CMP generated toward the later day of the culture due to additional level of spiked substrates (see Figure 4d), therefore in this case, required cells to express more metabolic enzymes to mediate the toxic effect of CMP. Altogether, the increasing level of gene expression of genes specifically involved in the pathway metabolizing metabolite CMP as shown here agreed with the previously shown experimental data where the concentration of CMP was found to be consistently high throughout during the entire culture duration, and therefore successfully validated the flux balance analysis results at using a simplified carbon utilization network level obtained from the flux modeling analysis study.

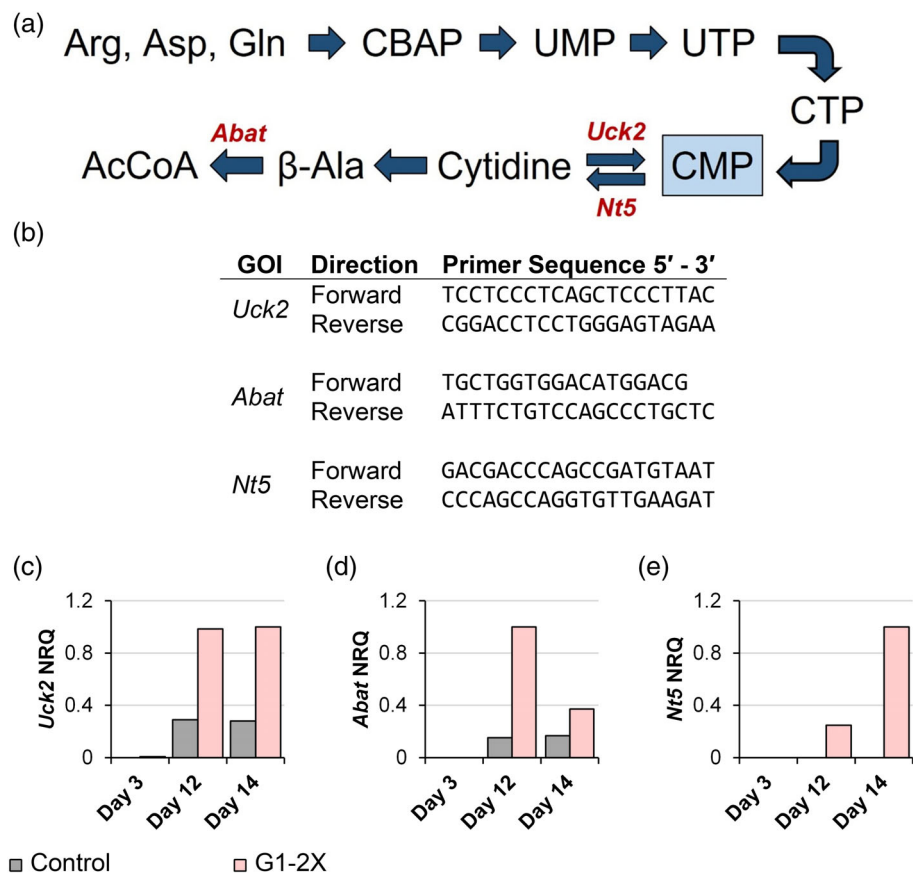


FIGURE 6 Gene expression analysis results from the dose-dependent nutrients spiking study. (a) Schematic diagram of cytidine monophosphate (CMP)-related metabolic pathway nested in the pyrimidine metabolism. (b) Target gene-of-interest (GOI) and corresponding forward and reverse primer sequence. Gene expression values of CMP-related genes: (c) *Uck2*, (d) *Abat*, and (e) *Nt5*. The gene expression of metabolic genes downstream to CMP was also evaluated via quantitative polymerase chain reaction. Gene expression values were presented as normalized relative quantification (NRQ) relative to the control and normalized using the min-max normalization method. *Abat*, aminobutyrate aminotransferase; AcCoA, acetyl coenzyme A; Arg, arginine; Asp, aspartate; CBAP, n-carbamoyl-l-aspartate; CMP, cytidine monophosphate; CTP, cytidine triphosphate; Gln, glutamine; *Nt5*, 5'-nucleotidase; *Uck2*, uridine-cytidine kinase 2; UMP, uridine monophosphate; β -Ala, β -alanine

3.6 | Design of medium optimizing study via *in silico* metabolic flux sensitivity analysis

As briefly mentioned, providing CHO cultures with nutrients rich medium can have a direct negative impact on cellular performance, mostly due to diversion of excess resources into inefficient pathways which can produce toxic by-products. Decreasing the level of amino acids supplemented to cells to only the amount required for growth and production, therefore, was postulated to have positive effect on cellular performance. One of the most difficult challenges in any medium optimization study is, perhaps, to rapidly screen for vital nutrients (that cannot be further optimized as any change will be detrimental to cells), or non-vital nutrients that are provided in excess and are non-beneficial to cells at their current supplemented level, before conducting any validation experiments. In this study, a rapid screening strategy was presented to explore the relationship between the concentration of the amino acids supplemented in the medium and their impact on growth through *in silico* simulation analysis. Since medium formulation was provided with enriched nutrients, the goal of this sensitivity analysis, therefore, was to quickly identify the lowest possible concentration of amino acids allowed without negatively impacting cellular biomass. Putative amino acids previously reported in the literature or were found in this study to interact with by-product inhibitory metabolite pathways were screened to evaluate their impact on growth. In this approach, flux balance analysis was performed at the genome-scale level on CHO-K1 cells based on the

metabolomic flux data obtained from the previously conducted fed-batch process. The uptake flux of each amino acid was subsequently decreased by 10%, 25%, 50%, and 75% one-by-one to determine the lowest achievable down-regulated factor that can be applied (see Figure 7a). The final lower limit thresholds for all amino acids at which their uptake fluxes can be reduced while still maintaining comparable growth rate to the control (no down-regulated factor applied) will be selected toward experimental medium optimization study.

The results of the sensitivity analysis study were shown in Figure 7b. Impact simulation study revealed three different case scenarios regarding decreasing the concentration of nutrients on cellular biomass generation. For case 1, the study identified vital nutrients such as arginine or glucose cannot have their supplemented concentration reduced to be less than the concentration found in the medium due to the observed negative impact on biomass. For case 2, the study showed important, but non-vital, nutrients such as glutamine or leucine can have their supplemented concentration reduced to a certain level before a negative impact on biomass production can be seen. For case 3, non-vital nutrients, such as aspartate or serine, were postulated to have their supplemented concentration reduced without showing any impact on cellular performance. Though this could hold true to a certain extent as these nutrients are non-essential and can be synthesized by cells as by-products from neighboring metabolic pathways (such as glycolysis or glycine biosynthesis); in reality, complete depletion of amino acids can have detrimental effects on cellular health and outweigh any potential benefit that can be gained

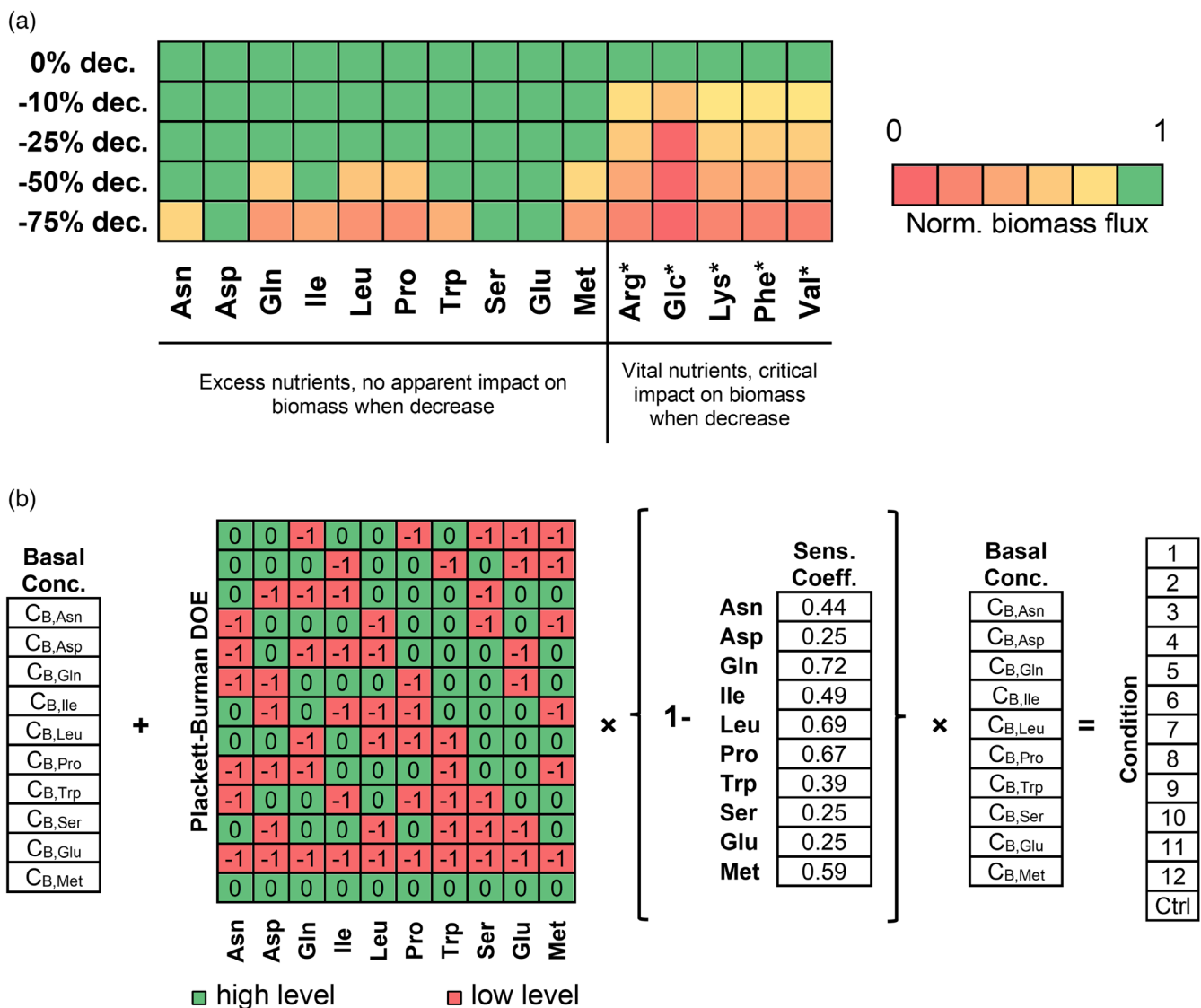


FIGURE 7 Sensitivity analysis and impact simulation screening of reducing amino acid for medium optimization study. (a) Pool of putative amino acid compounds explored in the sensitivity analysis study and impact screening results on generation of biomass due to decreasing amino acid uptake fluxes. (b) Target amino acids and Plackett-Burman screening design for optimizing the concentration of supplemented amino acids in the seed medium. For (a), each iteration started with a down-regulated factor (e.g., -10% decrease) applied to an individual amino acid, after which flux balance analysis was applied to recalculate production of biomass. Biomass flux was then normalized against that of the control condition (0% decrease) to determine the impact on growth in response to the imposed restriction of nutrients. For (b), the study was divided into 12 unique conditions with each condition exhibited a different linear combination of amino acids along with a negative control. The basal concentration of each amino acid was simultaneously varied to either high level (+, same concentration as found in the cultivated medium) or low level (-, with a down-regulated factor applied). *, vital nutrients that showed negative impact on growth profile upon removal and were not considered in further study; C_B, basal concentration; Sens. Coeff., sensitivity analysis coefficient

from reducing the secretion of toxic metabolites. Overall, the results of the study suggested 10 different amino acids including asparagine, aspartate, glutamine, isoleucine, leucine, proline, tryptophan, serine, glutamate, and methionine were provided in excess and might not all be required at the reported level to support growth and protein synthesis. In short, the sensitivity analysis study as shown here elucidated a sensible impact screening analysis prior to laboratory experiments that could rapidly scan for key critical medium components targeting reduction of generated toxic

metabolites by decreasing the amount of excess nutrients as found in the cultivated medium.

When considering decreasing the concentration of amino acids supplemented, complete dissolution of modified components needs to be carefully considered to avoid precipitation which can cause unwanted solids and negatively impact cell culture bioprocess.⁵ Since the utilized CHO culture medium as used throughout all experiments was intensified with concentrated nutrient components targeting to maximize resources use, the final down-regulated factors as studied

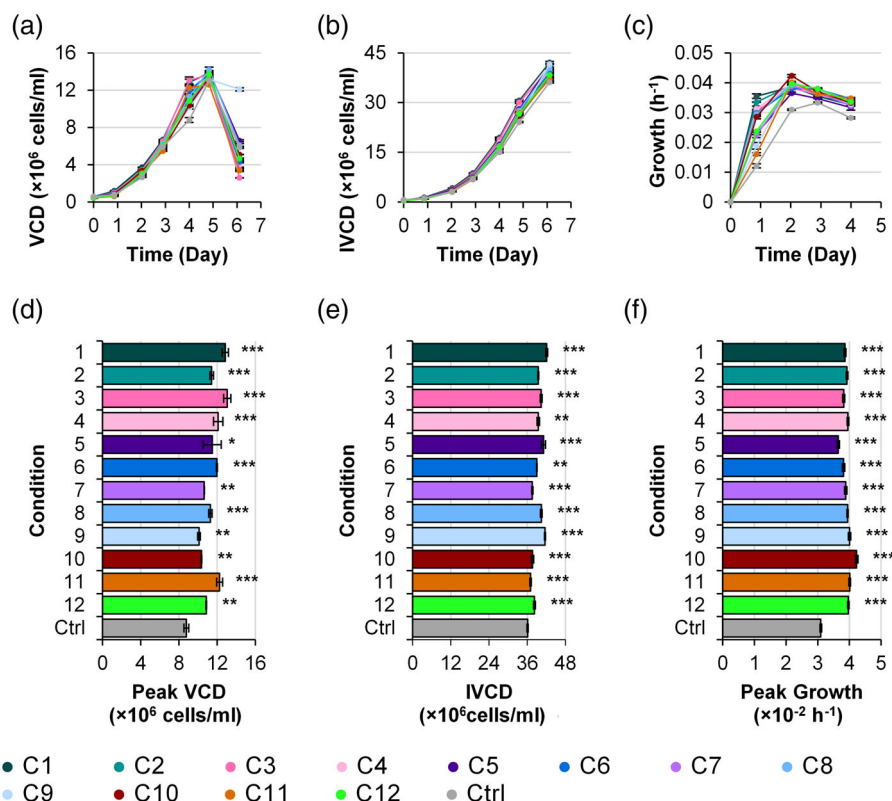


FIGURE 8 Cellular phenotype characteristic time-course profiles of batch CHO-K1 cells obtained from medium optimizing study. Time-course phenotype characteristic profiles: (a) viable cell density (VCD), (b) cumulative increase in integral viable cell density (IVCD), and (c) growth rate. Comparison of cellular performance across different experimental conditions against the control: (d) peak attainable VCD, (e) total cumulative IVCD, and (f) peak attainable growth rate. The study was divided into 12 unique conditions at different linear combination of amino acids along with a control. The supplemented concentration of each amino acid was simultaneously varied to either high level (same concentration as found in the control) or low level (less than the control) depending on the design of each condition. Cells from all conditions were derived from the same culture to eliminate variation in growth cycle and other culture conditions due to batch-to-batch variation; bars, mean \pm SD; $n = 3$; NS (statistically non-significant); * $p < 0.05$; ** $p < 0.01$; *** $p < 0.001$. Statistics by two-tailed t test

under this approach were slightly adjusted to allow complete dissolution of supplemented amino acids to the nutrient-lean medium without requiring the adjustment of medium pH which could affect osmolality and further introducing another variable in play. The final coefficient obtained from the sensitivity analysis study that can allow complete dissolution upon spiking into cell culture in later validation study were shown in Figure 7b.

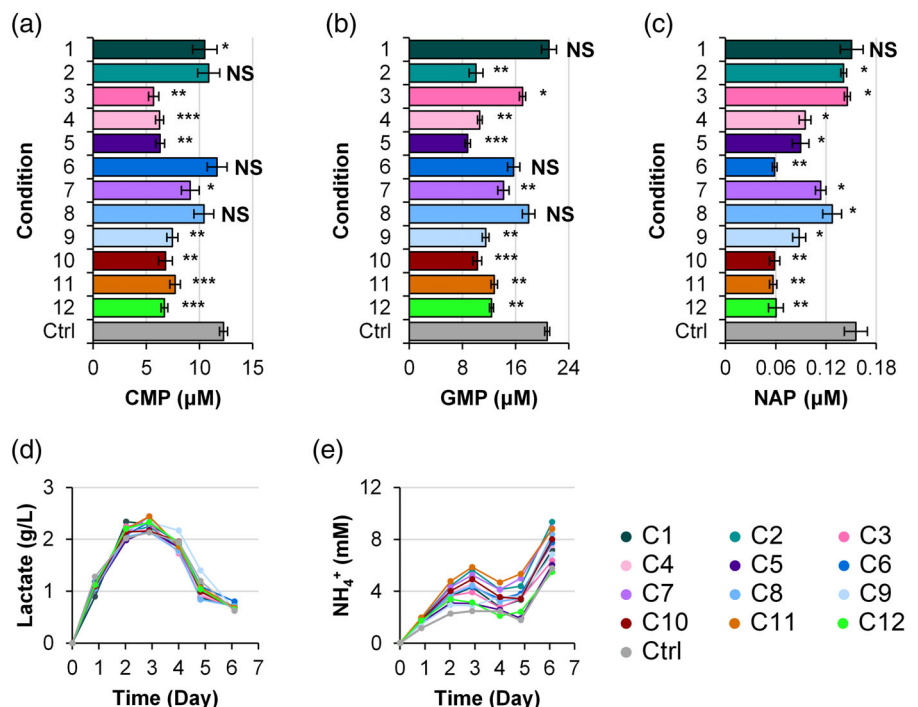
3.7 | Phenotype results of cells from medium optimizing study

A Plackett-Burman DOE design was incorporated to optimize medium components targeting cell expansion rate and peak achievable cell density in a CHO bioprocess (see Figure 7b). Two different types of mediums were obtained for this study: a modified amino acid-stripped medium, along with its non-modified counterpart (control). For those amino acids not considered in this study, their supplemented levels were added to the modified medium to the same level as the non-modified medium. Experimental design for each condition reflected the logics as presented in Figure 7b. For instance, the concentration of each amino acid from the control was kept the same as the basal medium concentration (C_B), and therefore can be expressed as: $1C_{B,Asn} + 1C_{B,Asp} + 1C_{B,Gln} + 1C_{B,Ile} + 1C_{B,Leu} + 1C_{B,Pro} + 1C_{B,Trp} + 1C_{B,Ser} + 1C_{B,Glu} + 1C_{B,Met}$. Condition 1 was then designed to screen for decreasing the concentrations of certain key amino acids: $1C_{B,Asn} + 1C_{B,Asp} + 0.72C_{B,Gln} + 1C_{B,Ile} + 1C_{B,Leu} + 0.67C_{B,Pro} + 1C_{B,Ser}$.

$0.25C_{B,Glu} + 0.59C_{B,Met}$. Each of the coefficient (e.g., $0.72C_{B,Gln}$) was carefully selected based on the results obtained from the *in silico* sensitivity analysis study. For example, sensitivity analysis on glutamine reported negative impact on biomass when glutamine was decreased to a fraction of 0.71 of the original concentration, and therefore the lowest achievable down-regulated factor for glutamine was set to 0.72 (i.e., $0.72C_{B,Gln}$). It is important to note that, although each condition as presented here represented a unique linear combination of amino acids, their overall supplemented concentrations would always be less than the control with no down-regulated factor applied. Thus, all 12 conditions as shown here allowed an exhaustive screening assessment on the potential benefits that can be gained from restricting excess nutrients diverting into non-optimal pathways.

Critical process performance (CPP) in terms of cellular phenotypic traits such as VCD profile, IVCD profile and growth rate obtained from the conducted batch process were systematically evaluated to assess the impact of each variable across all tested conditions (see Figure 8a-f). In general, all studied conditions with under-supplemented amino acids exhibited improved CPP characteristics over the control. When comparing the best performing condition at each CPP against the control, peak VCD profile of cells realized a 40% increase on Day 4 at 13.1×10^6 cells/ml (condition 3) versus 8.8×10^6 cells/ml (control). Similarly, the cumulative IVCD profile also realized a 15% increase on Day 6 at 6.1×10^6 cells/ml (condition 9) versus 36.1×10^6 cells/ml (control). Interestingly, the effect of down-supplementing amino acids realized by the best improvement in peak

FIGURE 9 Inhibitory metabolite profiles of batch CHO-K1 cells obtained from medium optimizing study. Inhibitory metabolites profiles at harvest day: (a) cytidine monophosphate (CMP), (b) guanosine monophosphate (GMP), and (c) n-acetylputrescine (NAP). Time-course inhibitory metabolite profiles: (d) lactate and (e) ammonia. The study was divided into 12 unique conditions at different linear combination of amino acids along with a control. The supplemented concentration of each amino acid was simultaneously varied to either high level (same concentration as found in the control) or low level (less than the control) depending on the design of each condition. Cells from all conditions were derived from the same culture to eliminate variation in growth cycle and other culture conditions due to batch-to-batch variation; bars, mean \pm SD; $n = 3$; NS (statistically non-significant); * $p < 0.05$; ** $p < 0.01$; *** $p < 0.001$. Statistics by two-tailed t test



growth rate calculated by a log-based growth model at 37% increase with the highest growing condition (condition 10) comparing against the control. Overall, improvement in cellular performance throughout the entire culture duration (Day 0 to Day 6) with respect to the target product CPP was realized across all studied conditions.

3.8 | Inhibitory metabolites profile of cells from medium optimizing study

Inhibitory metabolites profiles of cells obtained at harvest day were also reported (see Figure 9a–e). In general, restricting amino acids access from cells all resulted was found to be an effective strategy to control downstream accumulation of metabolic inhibitors (see Figure 9a–c). In general, any combination of down-regulating asparagine, aspartate, or glutamine (e.g., condition 1: $1C_{B,Asn} + 1C_{B,Asp} + 0.72C_{B,Gln}$, or condition 3: $1C_{B,Asn} + 0.25C_{B,Asp} + 0.72C_{B,Gln}$) all resulted in less secretion of metabolites CMP and GMP (all conditions, except condition 3). Interestingly, decreasing asparagine, aspartate, and glutamine all at once (condition 6) was shown to generate the lowest level of measured CMP and GMP. This observation as shown here was consistent with the results from dose-dependent nutrients spiking study, where increasing asparagine, aspartate and glutamine was found to induce formation of both CMP and GMP. On the other hand, decreasing proline, and to a certain degree asparagine, all resulted in lower concentration of measured NAP (condition 1, 6, 7, 8, 10, and 12). The results obtained here further strengthened the relationships between amino acids and metabolic inhibitors as demonstrated throughout this work. Interestingly, when investigating into the classically known and well-established process inhibitors such as lactate and ammonia, there was no significant difference in terms of the accumulation profile across all

conditions, including the control (see Figure 9d,e). However, cellular phenotype improvements were still observed (see Figure 8d–f), suggesting that decreasing amino acid concentrations to control metabolic resources diverting toward non-optimized inhibitory metabolite pathways such as CMP, GMP, and NAP can help improving process performance. The results from the study altogether confirmed significant fraction of fed nutrients was diverted into non-regulated metabolic pathways generating inhibitory by-products; and thus, by effectively limiting the amount of supplemented amino acid nutrients in the cultivated medium, the impacts of these identified rate-limiting factors were effectively controlled, allowing cells to achieve a higher growth rate and better overall peak and cumulative cell densities.

4 | CONCLUSION

In this study, the relationship between toxic metabolic inhibitors and their nutrient precursors was explored to identify the critical medium components toward cell growth and generation of metabolic by-products. Flux balance analysis study was conducted by mapping CMP, GMP, and NAP, all of which previously identified to generate from endogenous cell metabolism and verified to be toxic to cells, to a compartmentalized carbon utilization core model. Using this approach, the study projected high level of accumulation across all studied inhibitory metabolites when comparing two industrial relevant fed-batch feeding conditions, from which the results obtained were further validated via dose-dependent amino acids spiking study. In the end, a medium optimization design was employed to lower the amount of supplemented nutrients, of which improvements in critical process performance parameters were realized at 40% increase in peak VCD, 15% increase in IVCD and 37% increase in peak growth rate. Tight control of toxic

by-products was also achieved, as the study measured decreased inhibitory metabolites accumulation across all conditions. Altogether, this study presented a digital approach to investigate into the intertwined relationship between supplemented medium constituents and downstream toxic metabolites generating through host cell metabolism, which further elucidated different control strategies capable of improving cellular phenotypes and regulating toxic inhibitors.

AUTHOR CONTRIBUTIONS

Duc Hoang: Conceptualization (lead); data curation (lead); formal analysis (lead); investigation (lead); methodology (lead); validation (lead); writing – original draft (lead); writing – review and editing (lead). **Bingyu Kuang:** Conceptualization (lead); data curation (lead); formal analysis (lead); investigation (lead); methodology (lead); validation (lead); writing – original draft (lead); writing – review and editing (lead). **George Liang:** Data curation (lead); formal analysis (lead); investigation (lead); methodology (lead); writing – original draft (lead); writing – review and editing (lead). **Zhao Wang:** Conceptualization (equal); data curation (equal); formal analysis (equal); investigation (equal); methodology (equal); validation (equal); writing – original draft (equal); writing – review and editing (equal). **Seongkyu Yoon:** Funding acquisition (lead); investigation (lead); project administration (lead); resources (lead); supervision (lead); validation (lead); writing – original draft (lead); writing – review and editing (lead).

ACKNOWLEDGMENTS

This work was funded and supported by Advanced Mammalian Biomanufacturing Innovation Center (AMBIc) through the Industry – University Cooperative Research Center Program under U.S. National Science Foundation (Grant number: 1624684). We would like to express our gratitude to all AMBIc member companies for their mentorship and financial support. This work was conducted for a doctoral thesis and partially funded by The National Institute for Innovation in Manufacturing Biopharmaceuticals (NIIMBL, Grant/Award Number: 70NANB17H002).

CONFLICT OF INTEREST

The authors declare no conflict of interest.

PEER REVIEW

The peer review history for this article is available at <https://publons.com/publon/10.1002/btpr.3313>.

DATA AVAILABILITY STATEMENT

The data that support the findings of this study are available on request from the corresponding author. The data are not publicly available due to privacy or ethical restrictions.

ORCID

Duc Hoang  <https://orcid.org/0000-0002-7496-5193>

Seongkyu Yoon  <https://orcid.org/0000-0002-5330-8784>

REFERENCES

- Aggarwal S. What's fueling the biotech engine—2010 to 2011. *Nat Biotechnol.* 2011;29(12):1083-1089. doi:[10.1038/nbt.2060](https://doi.org/10.1038/nbt.2060)
- Cruz HJ, Freitas CM, Alves PM, Moreira JL, Carrondo MJT. Effects of ammonia and lactate on growth, metabolism, and productivity of BHK cells. *Enzym Microb Technol.* 2000;27(1-2):43-52. doi:[10.1016/S0141-0229\(00\)00151-4](https://doi.org/10.1016/S0141-0229(00)00151-4)
- Lao MS, Toth D. Effects of ammonium and lactate on growth and metabolism of a recombinant Chinese hamster ovary cell culture. *Biotechnol Prog.* 1997;13(5):688-691. doi:[10.1021/bp9602360](https://doi.org/10.1021/bp9602360)
- Mohmad-Saberi SE, Hashim YZHY, Mel M, Amid A, Ahmad-Raus R, Packeer-Mohamed V. Metabolomics profiling of extracellular metabolites in CHO-K1 cells cultured in different types of growth media. *Cytotechnology.* 2013;65(4):577-586. doi:[10.1007/s10616-012-9508-4](https://doi.org/10.1007/s10616-012-9508-4)
- Hoang D, Galbraith S, Kuang B, Johnson A, Yoon S. Characterization of Chinese hamster ovary cell culture feed media precipitate. *Biotechnol Prog.* 2021;37(5):e3188. doi:[10.1002/btpr.3188](https://doi.org/10.1002/btpr.3188)
- Mulukutla BC, Kale J, Kalomeris T, Jacobs M, Hiller GW. Identification and control of novel growth inhibitors in fed-batch cultures of Chinese hamster ovary cells. *Biotechnol Bioeng.* 2017;114(8):1779-1790. doi:[10.1002/bit.26313](https://doi.org/10.1002/bit.26313)
- Kuang B, Dhara VG, Hoang D, et al. Identification of novel inhibitory metabolites and impact verification on growth and protein synthesis in mammalian cells. *Metab Eng Commun.* 2021;13:e00182. doi:[10.1016/j.mec.2021.e00182](https://doi.org/10.1016/j.mec.2021.e00182)
- Feist AM, Herrgård MJ, Thiele I, Reed JL, Palsson BØ. Reconstruction of biochemical networks in microorganisms. *Nat Rev Microbiol.* 2009; 7(2):129-143. doi:[10.1038/nrmicro1949](https://doi.org/10.1038/nrmicro1949)
- Bordbar A, Monk JM, King ZA, Palsson BO. Constraint-based models predict metabolic and associated cellular functions. *Nat Rev Genet.* 2014;15(2):107-120. doi:[10.1038/nrg3643](https://doi.org/10.1038/nrg3643)
- Yusufi FNK, Lakshmanan M, Ho YS, et al. Mammalian systems biotechnology reveals global cellular adaptations in a recombinant CHO cell line. *Cell Syst.* 2017;4(5):530-542. doi:[10.1016/j.cels.2017.04.009](https://doi.org/10.1016/j.cels.2017.04.009)
- Selvarasu S, Ho YS, Chong WPK, et al. Combined *in silico* modeling and metabolomics analysis to characterize fed-batch CHO cell culture. *Biotechnol Bioeng.* 2012;109(6):1415-1429. doi:[10.1002/bit.24445](https://doi.org/10.1002/bit.24445)
- Yoon, S., B. Kuang, and D. Hoang, Cell Culture Methods. 2022, US Patent App. 17/671,029.
- Orth JD, Thiele I, Palsson BØ. What is flux balance analysis? *Nat Biotechnol.* 2010;28(3):245-248.
- Hefzi H, Ang KS, Hanscho M, et al. A consensus genome-scale reconstruction of Chinese hamster ovary cell metabolism. *Cell Syst.* 2016; 3(5):434-443. doi:[10.1016/j.cels.2016.10.020](https://doi.org/10.1016/j.cels.2016.10.020)
- Ahn WS, Antoniewicz MR. Parallel labeling experiments with [1, 2-13C] glucose and [U-13C] glutamine provide new insights into CHO cell metabolism. *Metab Eng.* 2013;15:34-47.
- Altamirano C, Cairo J, Godia F. Decoupling cell growth and product formation in Chinese hamster ovary cells through metabolic control. *Biotechnol Bioeng.* 2001;76(4):351-360.
- Hölttä E, Pohjanpeltö P. Polyamine dependence of Chinese hamster ovary cells in serum-free culture is due to deficient arginase activity. *Biochim Biophys Acta - Mol Cell Res.* 1982;721(4):321-327. doi:[10.1016/0167-4889\(82\)90085-4](https://doi.org/10.1016/0167-4889(82)90085-4)

SUPPORTING INFORMATION

Additional supporting information can be found online in the Supporting Information section at the end of this article.

How to cite this article: Hoang D, Kuang B, Liang G, Wang Z, Yoon S. Modulation of nutrient precursors for controlling metabolic inhibitors by genome-scale flux balance analysis. *Biotechnol Prog.* 2022;e3313. doi:[10.1002/btpr.3313](https://doi.org/10.1002/btpr.3313)